



Research Article

Insights into the Structural, Electronic, Optic, Elastic, and Phonon Properties of Half-Heusler Compound LiAgSe via Density Functional Theory

Sinem ERDEN GULEBAGLAN*¹

¹ Van Yüzüncü Yıl University, Van Vocational School, Department of Electric and Energy, 65080 Van, Turkey

Sinem ERDEN GULEBAGLAN, ORCID No: 0000-0001-9446-2211

*Corresponding author e-mail: sinemerden@gmail.com

Article Info

Received: 11.01.2022

Accepted: 10.03.2022

Online April 2022

DOI: 10.53433/yyufbed.1056381

Keywords

Dynamic properties,
Elastic properties,
Heusler crystal

Abstract: The structural, electronic, optic, elastic and dynamic features of LiAgSe half-Heusler structure are studied by using first principle calculations. LiAgSe half-Heusler compound is examined with the Generalized Gradient Approximation using the Density Functional Theory. The Quantum Espresso simulation program is preferred to investigate its structural, electronic and dynamic features. The ABINIT simulation program is preferred to investigate its elastic and optic properties. The electronic band structure graph of the LiAgSe crystal formed as a result of the calculation shows that this crystal has a semi-metallic structure. Optic properties such as, complex dielectric constant, extinction coefficient, reflectivity, for the volume of LiAgSe are calculated and plotted. In this study, elastic constants, Poisson's ratio and Debye Temperature values of LiAgSe half-Heusler crystal are determined. Apart from these, phonon dispersion curve graph is obtained. It has been calculated that the LiAgSe half-Heusler crystal is not dynamically stable in the ground state. However, when applied a pressure under nearly 16.396 GPa the crystal becomes stable.

Yoğunluk Fonksiyonel Teorisi Aracılığıyla Yarı-Heusler Bileşiği LiAgSe'nin Yapısal Elektronik Optik Elastik ve Fonon Özelliklerinin Tahmin Edilmesine İlişkin Öngörüler

Makale Bilgileri

Geliş: 11.01.2022

Kabul: 10.03.2022

Online Nisan 2022

DOI: 10.53433/yyufbed.1056381

Anahtar Kelimeler

Dinamik özellikler,
Elastik özellikler,
Heusler kristal

Öz: LiAgSe yarı-Heusler yapısının yapısal, elektronik, optik, elastik ve dinamik özellikleri ilk prensip hesaplamaları ile incelenmiştir. LiAgSe yarı-Heusler bileşiği, Yoğunluk Fonksiyonel Teorisi kullanılarak Genelleştirilmiş Gradient Yaklaşımı ile incelendi. Yapısal, elektronik ve dinamik özelliklerini araştırmak için Quantum Espresso simülasyon programı, elastik ve optik özelliklerini araştırmak için ise ABINIT simülasyon programı tercih edilmiştir. Hesaplama sonucunda oluşan LiAgSe kristalinin elektronik bant yapısı grafiği, bu kristalin yarı metalik bir yapıya sahip olduğunu göstermektedir. LiAgSe hacmi için kompleks dielektrik sabiti, extinction katsayısı, reflectivity, gibi optik özellikler hesaplandı ve çizildi. Bu çalışmada, yoğunluk fonksiyonel teorisi kullanılarak, LiAgSe yarı-Heusler kristalinin elastik sabitleri bulk, Poisson oranı ve Debye Sıcaklık değerleri belirlendi. Bu özelliklerin dışında fonon dağılım eğrisi LiAgSe yarı-Heusler kristalinin temel durumda dinamik olarak kararlı olmadığı, yaklaşık 16.396 GPa basınç altında kararlı bir şekilde dönüştüğü hesaplanmıştır.

1. Introduction

The discovery of Heusler compounds (Heusler, 1903) has had a significant impact on the development of new technological devices. When the studies in the literature are examined, Heusler compounds showing metal, semimetal or semiconductor properties can be found (Chiou et al., 2004; Erden Gulebaglan & Kilit Dogan, 2021a; Hadj et al., 2020; Kandpal et al., 2007; Huang et al., 2016; Zhang et al., 2020; Erden Gulebaglan & Kilit Dogan, 2021b; Abdullah et al., 2021; Asli et al., 2021; Kilit Dogan & Erden Gulebaglan, 2022). Half-Heusler compounds are structures that have the general formula XYZ. In general, X and Y elements in the formation of these structures are known as transition metals, and the Z element is known as the main group element (Graf et al., 2010). These structures are especially used in the production of power generation devices, thermoelectric devices and solid-state refrigerators (Riffat & Ma, 2003; Bell, 2008). Half-Heusler compounds are used in many fields such as topological insulators (Lin, 2010), superconductors (Benndorf et al., 2015; Winterlik et al., 2009), piezoelectric semiconductors, and thin-film solar cells, due to their wide variety of chemical compositions (Kacimi et al., 2014; Yang et al., 2017; Yin et al., 2019). There are studies in the literature that half-Heusler compounds are also suitable materials for spintronic applications (de Groot et al., 1983; Zuti et al., 2004; Boeck et al., 2002). Thermoelectric materials are used in order to save heat in exhaust and industrial systems (Yang & Stabler, 2009). The stability of Half-Heusler compounds at high temperatures makes them attractive materials for thermoelectric applications (Hassan & Ur, 2020). Fang et al. (2018) suggested that half-Heusler compounds with 8 or 18 valence electrons are candidates for thermoelectric applications due to their electrical properties, thermal stability and mechanical flexibility at high temperatures. Jia et al. (2021) investigated the thermoelectric properties of the CuLiX half-Heusler crystal with the deformation potential theory and semi-classical Boltzman theory. When the studies in the literature are analyzed, can be seen many studies investigating the properties of half-Heusler compounds and alloys containing lithium or silver or selenium. Zhang et al. (2003) computed the structural, electronic properties and spin magnetic moments of NiCrM (M=P, As, Sb, S, Se and Te) half-Heusler alloys. Ma et al. (2010) calculated the electronic and optical properties of LiGaS₂ and LiGaSe₂ crystals in orthorhombic phase using density functional theory. Wang et al. (2017) investigated the magnetic moments as well as the structural and electronic properties of LiCrZ (Z=S, Se, Te) alloys with the help of density functional theory. Özdemir and Merdan (2019), using density functional theory and Generalized Gradient Approach, MnZrIn, MnZrTl, MnZrC, MnZrSi, MnZrGe, MnZrSn, MnZrPb, MnZrSe etc. explained the electronic, magnetic and elastic properties of half-Heusler compounds. Zang and Xu (2020) developed the Gauss process regression model and estimated the lattice constants of many half-Heusler compounds. Dmytriv et al. (2011) investigated the LiAu₂In and Li_{0.65}Au_{0.05}In_{0.3} crystals experimentally and determined the crystal structure properties of these structures, namely their atomic parameters and Wyckoff positions. Casper et al. (2009) stated that in LiGaGe half-Heusler compound, GaGe hexagonal layers can become semiconductor depending on the degree of shrinkage. Hussain (Hussain, 2018) analyzed the magnetic and electronic properties of newly (001) surfaced LiCrSe and LiCrS half-Heusler crystals using density functional theory. Telfah et al. (2021) declared the electronic structures, magnetic and thermoelectric properties of KCrS, KCrSe and KCrTe half-Heusler crystals. Berger and Weiss (1988) investigated the crystal properties of Ag-Mg-RE (RE= La, Ce, Pr, Nd, Sm) Heusler phase crystals experimentally. Jolayemi et al. (2021) determined the thermoelectric properties of LiAlSi crystal using Boltzmann transport theory and density functional theory. Kilit Dogan and Erden Gulebaglan (2021) analyzed and declared the electronic, elastic and dynamic properties of LiInSi crystal using density functional theory.

The aim of this study is to obtain information about the structural, electronic, optic, elastic and dynamic properties of the LiAgSe crystal before it is synthesized in the laboratory. The first goal of the study was to determine the structural and electronic properties of the LiAgSe Heusler compound. As a second step, the analysis of the optic, elastic and dynamic properties of the LiAgSe compound was performed. To date, no study has been found showing that comprehensive research has been done on the LiAgSe crystal. For this reason, the results obtained for the LiAgSe half-Heusler compound will contribute to the literature for the first time.

2. Material and Methods

Although it has not been synthesized in a laboratory yet, many of the physical properties of a crystal structure can be studied by a simulation. The results obtained are predictions for the researchers before their experimental studies. This provides advantages relevant to cost and time. Two of these simulation programs are the Quantum Espresso (PWSCF) (Giannozzi et al., 2009) simulation package program and the ABINIT (Gonze et al., 2002) program. The structural, electronic and dynamic properties of the LiAgSe half-heusler crystal were calculated with the Quantum Espresso program, while the elastic and optic properties were examined with the ABINIT program. The Quantum Espresso and ABINIT programs are based on the density functional theory and the properties of the LiAgSe crystal were calculated using the Generalized Gradient Approximation (Perdew & Zunger, 1981). In the Generalized Gradient Approximation, the exchange correlation interaction was expressed in the calculations with the help of the Perdew Burke Ernzerhof (Perdew et al., 1997) function. With a cutoff energy of 100 Ry (for both simulation programmes), the plane wave expansion of the Kohn-Sham (1965) wave functions was limited. For charge density, this value was taken as 400 Ry. When examining all the properties of the LiAgSe half Heusler compound, the Brillouin region was represented by the Monkhorst-Pack (1976) as a $14 \times 14 \times 14$ k -point. The valence electrons for the LiAgSe unit cell are $2s^1$ of Li, $4d^{10} 5s^1$ of Ag, $3d^{10} 4s^2 4p^4$ of Se. The dynamic properties of the LiAgSe half-Heusler compound were investigated by Linear-Response method. Dynamic matrices were determined by using Brillouin region $4 \times 4 \times 4$ q -points in the calculation of dynamic properties. Spin-orbit interaction was not taken into account in all calculated properties of the LiAgSe half-Heusler compound.

3. Results

In this study, initially, the structural properties of the LiAgSe compound with the space group $F\bar{4}3m$ (No:216) were explored. The coordinates of the three atoms that composed the LiAgSe half-Heusler compound are 0.25, 0.25, 0.25 (Li), 0.50, 0.50, 0.50 (Ag) and 0.00, 0.00, 0.00 (Se). The Vesta program was used to envision the LiAgSe half-Heusler compound. The crystal structure of the LiAgSe compound was demonstrated in Figure 1. As seen from Figure 1, there are bonds between Li-Ag, Ag-Se and Li-Se atoms. The bond lengths are calculated and given in Table 1.

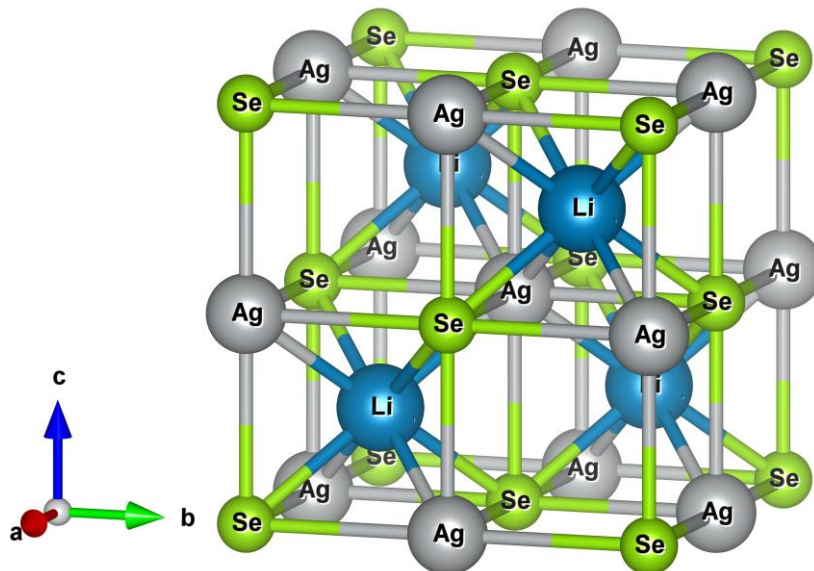


Figure 1. Representation of the crystal structure of Half-Heusler LiAgSe compound.

Table 1. The bonds and bond lengths for the LiAgSe compound

Bonds	Bond Lengths (Å)
Li-Ag	2.63
Ag-Se	3.04
Li-Se	2.63

After the cutoff energy test and the k-point value test for LiAgSe half-Heusler compound, ground state energy values were determined against different volume values. These values were fitted to the Vinet (1986) equation and the lattice constant of the LiAgSe half-Heusler compound was calculated. The lattice parameter value for the LiAgSe half-Heusler compound was computed as $a_{\text{LiAgSe}} = 6.09 \text{ \AA}$ in this study. The calculated lattice parameter value of the LiAgSe crystal is in good agreement with the previous result (Jain et al., 2013). Gruhn (2010) found the lattice constant of LiAgSe crystal in half Heusler structure to be 6.259 \AA . Lekhal et al. (2016) suggested that cubic XYZ compounds with C1b structure crystallize in space group $F\bar{4}3m$ (No:216) in zincblende structure type with close cubic cell parameters of 6.0 \AA . The calculated lattice parameter value with the suggestion of Lekhal et al. (2016) was consistent. Electronic band structure was figured out by using the computed lattice parameter value for LiAgSe half Heusler compound. Figure 2 shows the electronic band structure of LiAgSe half-Heusler compound.

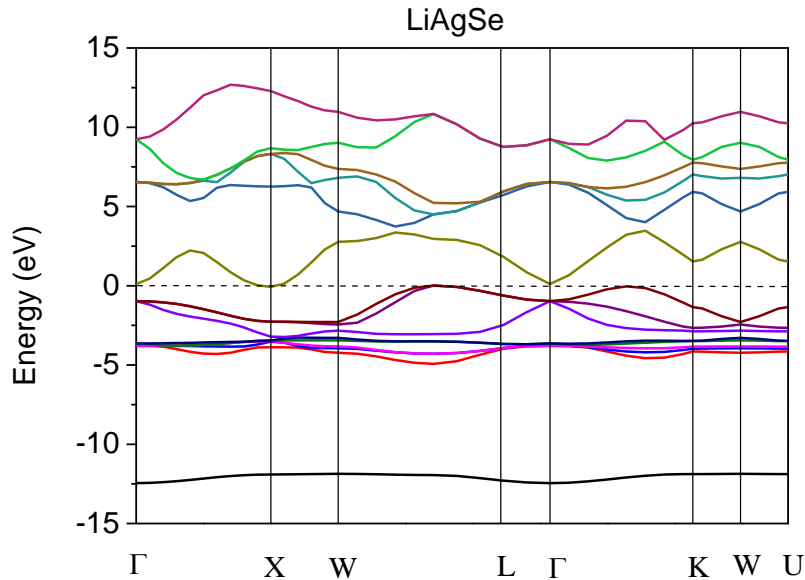


Figure 2. Electronic band structure for half-Heusler LiAgSe.

The electronic band structure of LiAgSe is plotted along for some high symmetry points which are given in Figure 2 at zero Kelvin. LiAgSe crystal shows semi-metals properties. It has been concluded that the lowest level of the conductivity band and the highest level of the valence band are intervened at a value of approximately -0.1 eV . The region where this interlocking takes place is between the X high symmetry point and the W-L high symmetry points. Afterwards, the total and partial densities of the states given in Figure 3 were calculated and plotted. Figure 3(a) shows the contributions of Li atoms to the density of states. These contributions mainly originate from the conduction bands with p states but there are slight contributions from s and d states also from valence bands. The contribution of Ag atom is just from the valence bands with d states. The contribution of Se atom is mainly from the core electrons with s states and a small contribution is from valence bands with p states.

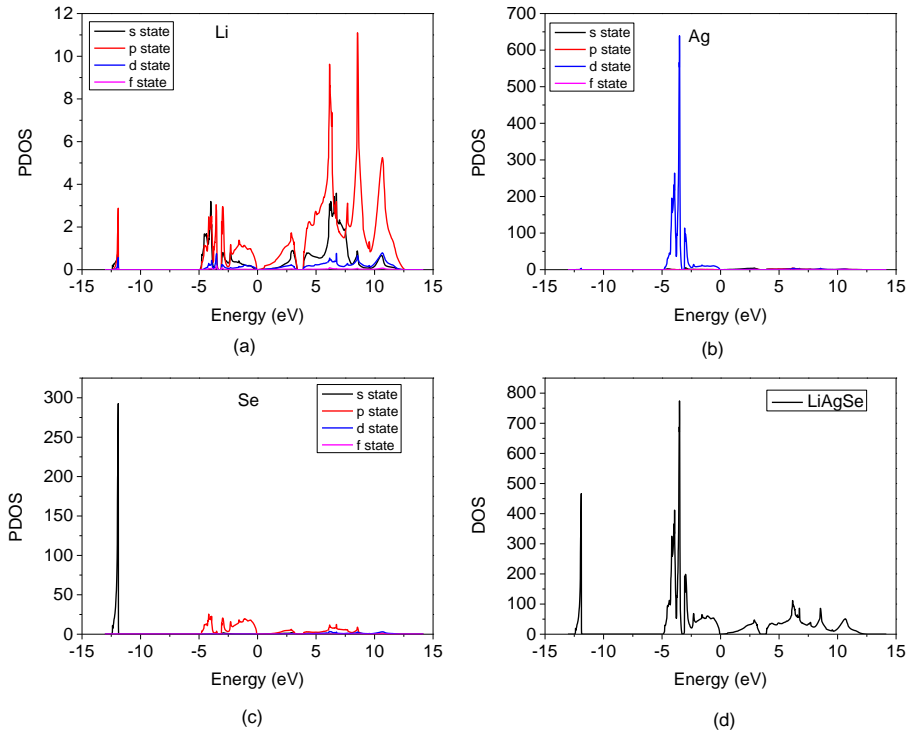


Figure 3. Partial density of states of (a) Li, (b) Ag, (c) Se atoms and (d) Total density of states of LiAgSe compound.

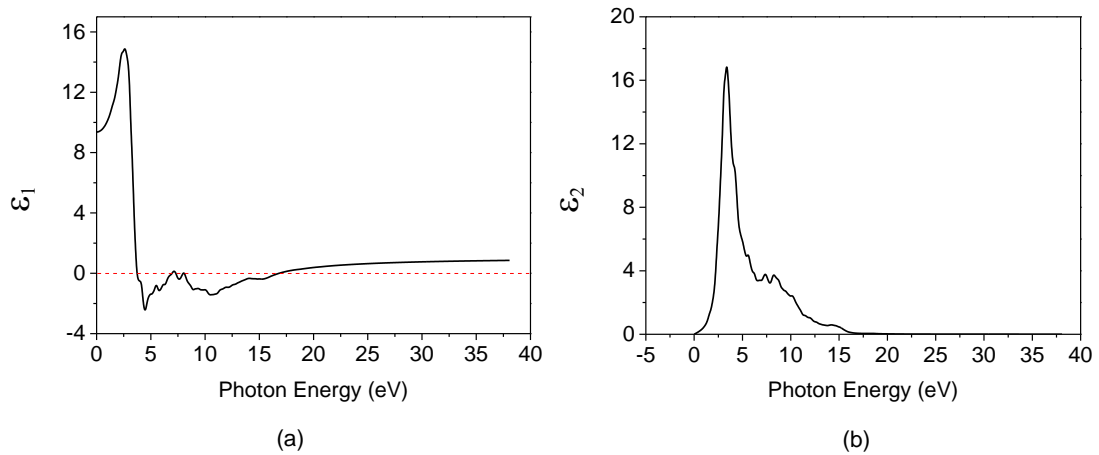


Figure 4. (a) Real and (b) Imaginary part of complex dielectric function of LiAgSe.

In the literature, there are studies examining the optical properties of materials with semimetal properties (Rahman Rano et al., 2020; Homes et al., 2015). Our next aim was to compute the optic properties of LiAgSe compound. Therefore, the real (ϵ_1) and complex (ϵ_2) parts of the dielectric function were calculated and plotted (Figure 4). The complex part of the dielectric function was calculated first, and the real part could be calculated by using the complex part of the dielectric function by using the Kramers-Kronig equations. Figure 4 (a) shows that between 3.68 and 16.84 eV values except for the two peak points at 7.09 eV and 7.99 eV the real part takes negative values. This negative part shows the reflection of the light. This range is also consistent with the reflection graph of the LiAgSe compound given in Figure 5 (c). The two peak points mentioned above correspond to the minimum points of the

reflection graph with the same energy values refer to the plasmon excitations. The other energy values for the plasmon excitations are 3.68 eV and 16.84 eV. In other words at the energy values at which the real part of the dielectric function takes zero value, plasmon excitations occur. The static dielectric constant (ϵ_0) is the value of the real part with zero energy which is equal to 9.39 for the LiAgSe compound. The complex part of the dielectric function gives information about the electron transitions around the band gap. In addition, extinction coefficient, refractive index, reflectivity, effective number of valence electrons per unit cell, absorption and energy loss functions were calculated and plotted for LiAgSe volume (Figure 5). The static refractive index, $n(0)$ is calculated as 3.06 for the LiAgSe compound from Figure 5 (a). N_{eff} is also related to the transition between the bands. Since the N_{eff} value saturates after 16 eV, no transitions can be observed between the bands with the values bigger than 16 eV as shown in Figure 5(d). The absorption coefficient (α) (Figure 5e) is also in good agreement with the other optic properties calculated in this study.

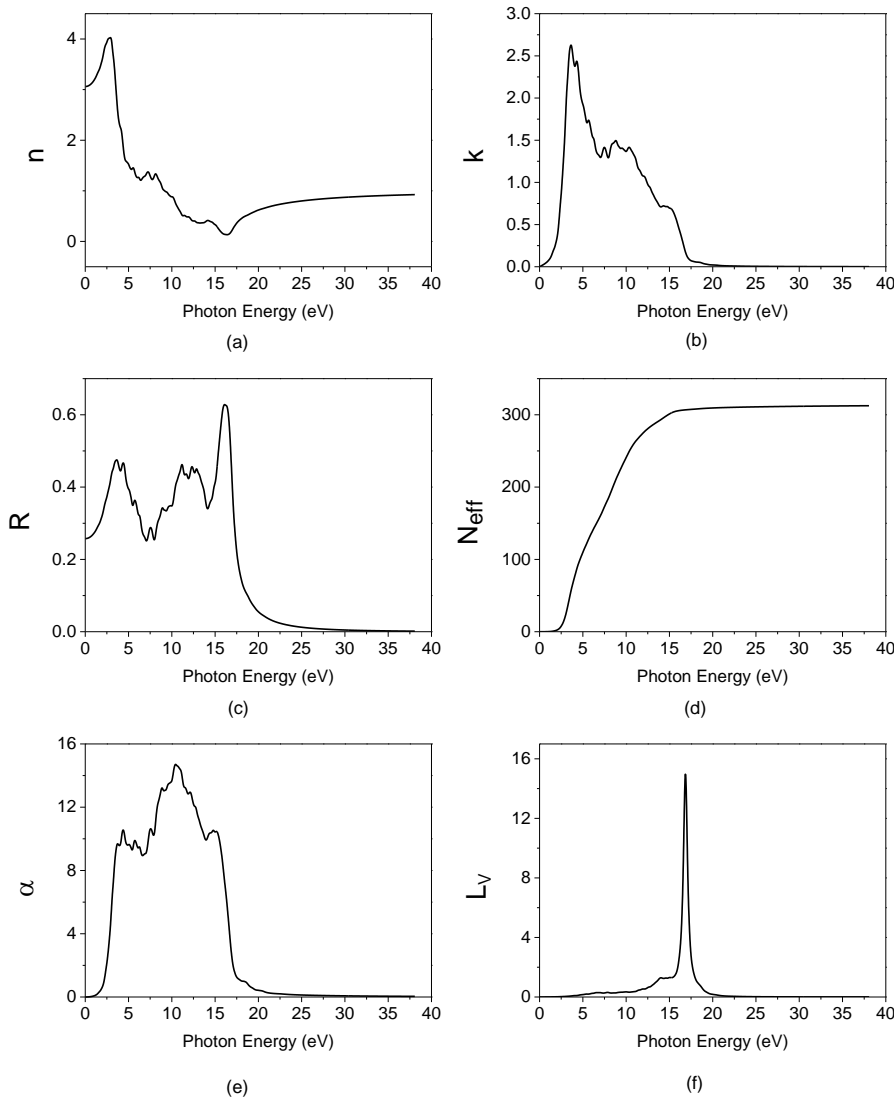


Figure 5. (a) Refractive index, (b) Extinction coefficient, (c) Reflectivity, (d) Effective number of valence electrons per unit cell, (e) Absorption and (f) Energy loss function for the volume of LiAgSe.

The energy loss function for volume, L_V , refers to the missing energy of a transition electron. From the first L_V values (which are different from zero) to the peak value are related to the plasma

oscillations. These values are around 3 to 16 eV which is consistent with the negative value portion of the real part of the dielectric function.

In order to examine the elastic properties of the LiAgSe semi-Heusler compound, elastic stiffness (C_{ij}) constants were calculated using the density functional theory through the general gradient approximation with the help of the ABINIT program. It is a tensor (C_{klmn}) whose elastic stiffness constants are of rank=4. This tensor can be represented as C_{ij} using matrix notation and the number of components of the tensor is reduced from 81 to 36 (Nye, 1995). The LiAgSe half-Heusler compound has a cubic structure. Due to the symmetrical property of cubic structures, the number of dependent components is 12. These dependent variables are $C_{11}=C_{22}=C_{33}$, $C_{44}=C_{55}=C_{66}$ and $C_{12}=C_{13}=C_{21}=C_{23}=C_{31}=C_{32}$. Also the number of independent components is 3. These parameters are C_{11} , C_{12} , and C_{44} . The values of the independent elastic stiffness constants of LiAgSe half-Heusler are given in Table 2. For a mechanically stable material, the Innate Stability Criteria (Mouhat and Coudert, 2014) and the elastic stiffness constants must comply. These criteria for cubic structure are given below (equation1).

$$C_{11} > 0, C_{12} < B < C_{11} \text{ and } C_{44} > 0 \quad (1)$$

Here B is the Bulk modulus. The LiAgSe half-Heusler is mechanically stable since it satisfies the Innate Stability Criteria.

Table 2. The values of elastic stiffness constants of LiAgSe half-Heusler compound

LiAgSe	C_{11} (GPa)	C_{12} (GPa)	C_{44} (GPa)
Ground state (P=0 kbar)	42.57	44.16	26.18

Bulk modulus (B), Shear Modulus (G) values were calculated by Voigt (Voigt, 1889), Reuss (Reuss, 1929) and Hill (Hill, 1966) approximations. Based on these calculated values, Young's modulus (E), Poisson ratio and Debye Temperature values were obtained. These calculations were made with elastic stiffness constants. All the results obtained are given in Table 3.

Table 3. Values of some elastic features of LiAgSe half-Heusler compound

Elastic Properties of LiAgSe	Symbol (unit)	Values
Bulk Modulus	B_V (GPa)	43.63
Shear Modulus	G_V (GPa)	15.39
Young Modulus	E (GPa)	19.01
Poisson Ratio	ν (-)	0.43
Debye Temperature	Θ_D	45.79

Bulk modulus is a property of a material indicating its degree of resistance to compression. A material's high modulus of bulk means that it has high resistance to compression. The low bulk modulus indicates that it can be compressed easily. It was calculated that the LiAgSe crystal whose properties were examined has a not very high bulk modulus value. This means that the LiAgSe crystal can be easily compressed.

If the value of the Poisson's ratio is less than 0.26, it is said that this material is fragile. The calculated Poisson's ratio is obtained as 0.43, which is greater than 0.26. This result gives the information shows that the LiAgSe half-Heulser compound has a very elastic structure. By calculating the Debye temperature of a crystal, information about the thermal conductivity of that crystal can be obtained. Briefly, Debye temperature values are related to the thermal conductivity property of a material. Based on the literature, it can be said that materials with good thermal conductivity are crystal structures with Debye temperatures above 80 K (Kilit Dogan & Erden Gulebaglan, 2022). The Debye temperature is calculated as 45.79, which is not very high. Therefore, LiAgSe has a thermal conductivity

property but not very high. This result is also compatible with the phonon dispersion results mentioned below.

Next, the phonon properties of the LiAgSe compound were investigated. In the base case, the dispersion and density of states of the phonons given in Fig. 6 and Fig. 7, respectively, were calculated and plotted.

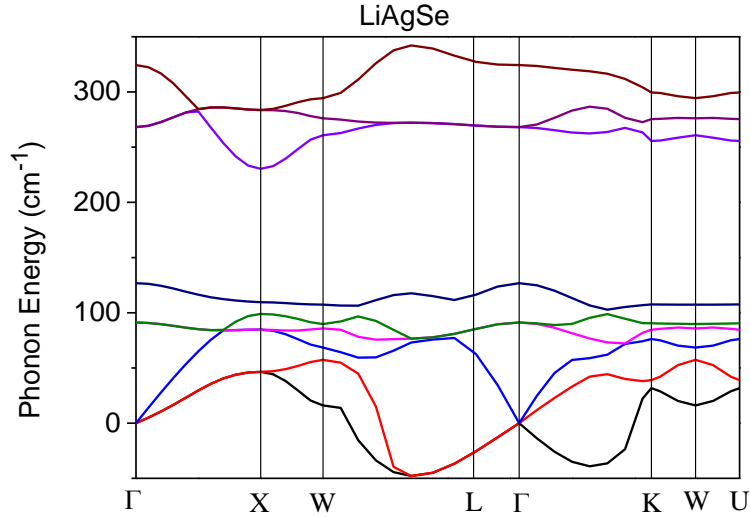


Figure 6. Phonon dispersion graph of LiAgSe in the ground state.

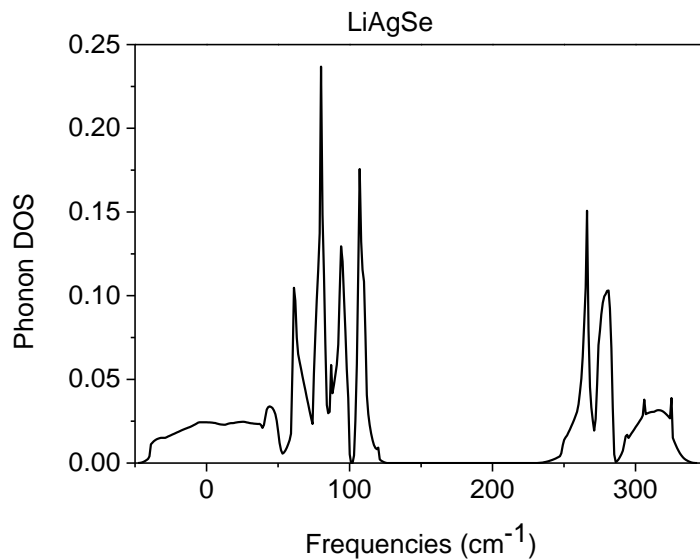


Figure 7. Phonon density of states graph of LiAgSe in the ground state.

LiAgSe has 3 atoms in its unit cell, so 9 phonon modes occur. Three of them with the lowest (here negative) frequencies are acoustic modes and the rest of the six are optic modes (Figure 6). For both types of modes (acoustic and optic) there are transverse and longitudinal modes. Because the vibration takes place on a plane. One of the modes occurring in that plane is called the transverse mode (transverse acoustic, TA or transverse optic, TO). Since there are possibly three vibration planes, two of them are out of the vibration plane. One of the out-of-plane modes is again the transverse mode, and the last one is the longitudinal mode (longitudinal acoustic LA, or longitudinal optic LO). The transverse modes have lower frequencies than longitudinal mode. Examining Figure 6, it is seen that the acoustic modes have negative frequencies, indicating that this material is dynamically unstable in the ground

state. If two or more modes overlaps for some regions this situation is called degeneracy. High degeneracy points out that this material has high symmetry properties. Again, looking at Figure 6, it is seen that the degeneracy is not high enough for a stable material. At this point, it was wondered whether there was a pressure value stabilizing this material dynamically when applied. After calculations, it was found that LiAgSe becomes dynamically stable if a pressure of 16,396 GPa is applied. Both phonon graphs were drawn under this pressure value (Figure 8 and Figure 9).

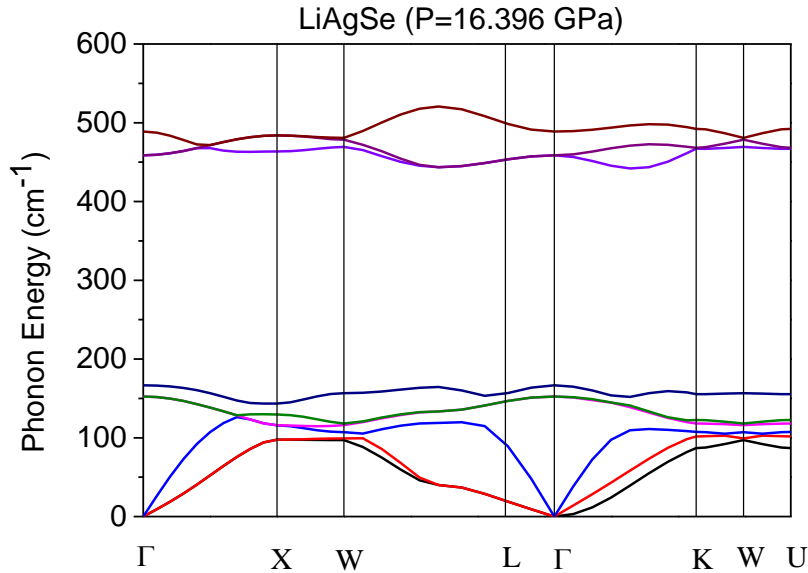


Figure 8. Phonon dispersion graph of LiAgSe under pressure (P=16.396 GPa).

Figure 8 and Figure 9 shows that acoustic modes have zero frequency as they are supposed to be. Now, Figure 8 and Figure 9 can be studied in depth. In Figure 8, the two modes with the very lowest frequencies are transverse acoustic modes. The third mode is the longitudinal acoustic mode. These three modes have zero frequency for the Γ high symmetry point. TA modes have high degeneracy. After LA mode, two TO modes appear with high degeneracy. The LO mode appears next to the TO modes. There is also a second group of phonon bands between 440-520 cm⁻¹ frequency values. There are three optic modes. Two of them with lower frequencies are TO modes the last of which is LO mode. Here, there is a high degeneracy between TO modes in this group of phonon modes

By examining the TA modes of a material, one can get an idea about the thermal conductivity of a material. TA modes are directly related to the thermal conductivity of that material. If there is no scattering between the TA modes then these materials are said to have a high thermal conductivity. If TA modes and TO modes coincide together, scattering in the TA modes occur, and thermal conductivity decreases. When examining it is understood that TO and TA modes do not overlap under both the ground state and at the pressure level P=16.396 GPa. So it can be concluded that LiAgSe has a thermal conductivity property but Figure 6 and Figure 8 show that this property has increased with the applied pressure. Also the Debye temperature value calculated within the elastic properties is coherent with this result.

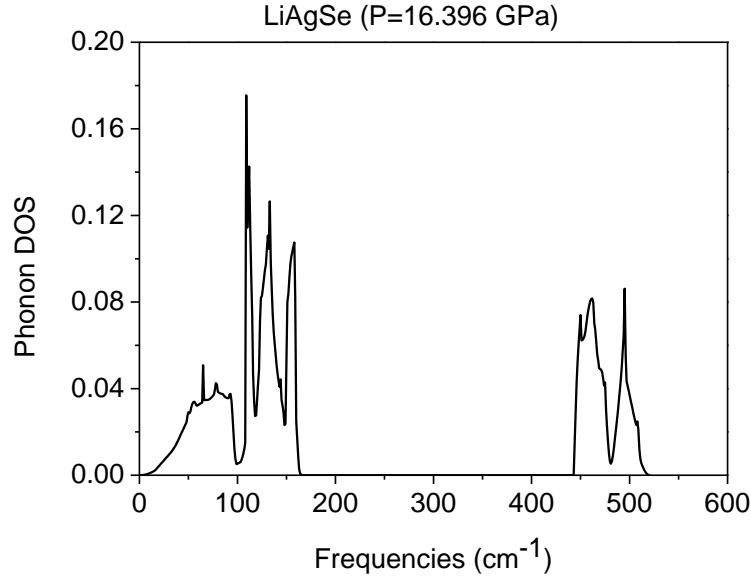


Figure 9. Phonon density of states graph of LiAgSe under pressure (P=163.96 kbar)

It was found the irreducible representation of Γ by a factor analysis using the Bilbao Crystallographic Server (Aroyo et al., 2006). The space group of LiAgSe is $F\bar{4}3m$ (No:216) and its point group is T_d ($\bar{4}3m$). For materials in this group the symmetry types are A_1 , A_2 , E , T_1 and T_2 . It was calculated and there presentation is as follows (equation2, equation3 and equation 4)

$$\Gamma = \Gamma_{ac} + \Gamma_{op} \quad (2)$$

$$\Gamma_{ac} = T_2 \quad \text{and} \quad \Gamma_{op} = 2T_2 \quad (3)$$

$$\Gamma = 3T_2 \quad (4)$$

It has been seen that the $2T_2$ (without acoustic modes) belongs to Infrared active, Raman active and Hyper-Raman active modes.

4. Discussion and Conclusion

Structural, electronic, optic, elastic and phonon properties of the LiAgSe half-Heusler compound were discussed with the help of Density Functional Theory and Quantum Espresso and ABINIT programs using Generalized Gradient Approximation. The ABINIT program was used to investigate the optic and elastic properties of LiAgSe half-Heusler compound, and Quantum Espresso computer program was used for searching structural, electronic and phonon properties. The lattice parameter value of the LiAgSe half-Heusler compound was calculated and compared with the literature and they were found to be compatible. When the electronic properties of the compound were examined, it was concluded that LiAgSe is a semi-metal. Afterwards, it was investigated the optical properties of the LiAgSe compound. The complex dielectric function was calculated and given with graphs. Also, all calculated optic properties of the LiAgSe are given in the graphs and are compatible with each other. Next, the elastic properties of LiAgSe semi-Heusler compound were focused on. The main constants of elasticity of the studied compound were calculated. It is seen that this material is a very elastic material. Last of all, the phonon properties of the LiAgSe compound were investigated. It is obvious that this material is not dynamically stable in the ground state. It becomes stable under a pressure value of $P=16.396$ GPa. The thermal conductivity property occurs but it is not very high for the ground state, it increases with the pressure. Irreducible representations of Γ were also obtained. It is believed that this detailed study on the LiAgSe semi-Heusler compound will assist researchers in their future work on LiAgSe semi-Heusler compounds.

References

- Abdullah, A., Husain, M., Rahman, N., Khan, R., Iqbal, Z., Zulfiqar, S., Sohail, M., Umer, M., Murtaza, G., Khan, S. N., Khan, A., & Reshak, A. H. (2021). Computational investigation of structural, magnetic, elastic, and electronic properties of Half-Heusler ScVX (X = Si, Ge, Sn, and Pb) compounds. *European Physical Journal Plus*, 136, 1176. doi: 10.1140/epjp/s13360-021-02175-4
- Aroyo, M. I., Perez-Mato, J. M., Capillas, C., Kroumova, E., Ivantchev, S., Madariaga, G., & Kirov, A. (2006). Bilbao Crystallographic Server: I. Databases and crystallographic computing programs. *Zeitschrift für Kristallographie*, 221(1), 15-27. doi: 10.1524/zkri.2006.221.1.15
- Asli, N., Dahmane, F., Mokhtari, M., Zouaneb, C., Batouche, M., Khachai, H., Srivastava, V., Naqib, S. H., Al-Douri, Y., Bouhemadou, A., & Khenata, R. (2021). Structural, electronic, magnetic and mechanical properties of the full-Heusler compounds Ni₂Mn (Ge, Sn) and Mn₂NiGe. *Zeitschrift für Naturforschung A*, 76(8), 693-702. doi: 10.1515/zna-2020-0329
- Bell, L. E. (2008). Cooling, heating, generating power, and recovering waste heat with thermoelectric systems. *Science*, 321, 1457-1461. doi: 10.1126/science.1158899
- Benndorf, C., Niehous, O., Eckert, H., & Tanko, O. (2015). ²⁷Al and ⁴⁵Sc NMR spectroscopy on ScT₂Al and Sc (T_{0.5}T'_{0.5})₂Al (T = T' = Ni, Pd, Pt, Cu, Ag, Au) heusler phases and superconductivity in Sc (Pd_{0.5}Au_{0.5})₂Al. *Zeitschrift für Anorganische und Allgemeine Chemie*, 641(2), 168. doi: 10.1002/zaac.201400509
- Berger, G., & Weiss, A. (1988). Ternary intermetallic phases with Heusler-phase type structures in the system Ag-Mg-RE (RE = La, Ce, Pr, Nd, Sm). *Journal of the Less-Common Metals*, 142, 109-121. doi: 10.1016/0022-5088(88)90168-3
- Boeck, J. D., Roy, W. V., Das, J., Motsnyi, V., Liu, Z., Lagae, L., Boeve, H., Dessein, K., & Borghs, G. (2002). Technology and materials issues in semiconductor-based magnetoelectronics. *Semiconductor Science and Technology*, 17(4), 342. doi: 10.1088/0268-1242/17/4/307
- Casper, F., Seshadri, R., & Fesler, C. (2009). Semiconducting half-Heusler and LiGaGe structure type compounds. *Physica Status Solidi A*, 206(5), 1090. doi: 10.1002/pssa.200881223
- De Groot, R. A., Mueller, F. M., Van Engen, P. G., & Buschow, K. H. J. (1983). New class of materials: half-metallic ferromagnets. *Physical Review. Letter*, 50(25), 2024. doi: 10.1103/PhysRevLett.50.2024.
- Dmytriv, G. S., Pavlyuk, V. V., Pauly, H., Eckert, J., & Ehrenberg, H. (2011). New real ternary and pseudoternary phases in the Li-Au-In system. *Journal of Solid State Chemistry*, 184, 1328. doi: 10.1016/j.jssc.2011.03.020
- Erden Gulebaglan, S., & Kilit Dogan, E. (2021a). Investigation of structural, electronic, and dynamic properties of half-Heusler alloys XCuB (X = Ti, Zr) by first principles calculations. *Crystal Research and Technology*, 56(1), 2000116. doi: 10.1002/crat.202000116
- Erden Gulebaglan, S., & Kilit Dogan, E. (2021b). A comparison study of the structural electronic, elastic and lattice dynamic properties of ZrInAu and ZrSnPt. *Zeitschrift für Naturforschung A*, 76, 6, 559. doi: 10.1515/zna-2021-0014
- Fang, T., Zhao, X., & Zhu, T. (2018). Band structures and transport properties of high-performance half-Heusler thermoelectric materials by first principles. *Materials*, 11, 847. doi: 10.3390/ma11050847
- Giannozzi, S., Bonini, N., Calandra, M., Car, R., Cavazzoni, C., Ceresoli, D., Chiarotti, G. L., Cococcioni, M., Dabo, I., Corso, A. D., de Gironcoli, S., Fabris, S., Fratesi, G., Gebauer, R., Gerstmann, U., Gougoussis, C., Kokalj, A., Lazzeri, M., Samos, L. M., Marzari, N., Mauri, F., Mazzarello, R., Paolini, S., Pasquarello, A., Paulatto, L., Sbraccia, C., Scandolo, S., Sclauzero, G., Seitsonen, A. P., Smogunov, A., Umari, P., & Wentzcovitch, R. M. (2009). QUANTUM ESPRESSO: a modular and open-source software project for quantum simulations of materials. *Journal of Physics: Condensed Matter*, 21, 395502. doi: 10.1088/0953-8984/21/39/395502
- Gonze, X., Beuken, J. M., Caracas, R., Detraux, F., Fuchs, M., Rignanese, G. M., Sindic, L., Verstrate, M., Zerah, G., Jollet, F., Torrent, M., Roy, A., Mikami, M., Ghosez, P., Raty, J. Y., & Allan, D. C. (2002). First-principle computation of material properties: the ABINIT software project. *Computational Materials Science*, 25, 478. doi: 10.1016/S0927 0256(02)00325-7

- Graf, T., Parkin, S. S., & Fesler, C. (2010). Heusler compounds-a material class with exceptional properties. *IEEE Transactions on Magnetics.*, 47, 367-373. doi: 10.1109/TMAG.2010.2096229
- Gruhn, T. (2010). Comparative ab initio study of half-Heusler compounds for optoelectronic applications. *Physical Review B* 82: 125210. doi: org/10.1103/PhysRevB.82.125210
- Hadj, T., Khalfoun, H., Rached, H., Guermit, Y., Azzouz-Rached, A., & Rached, D. (2020). DFT study with different exchange-correlation potentials of physical properties of the new synthesized alkali-metal based Heusler alloy. *European Physical Journal B*, 93, 214. doi: 10.1140/epjb/e2020-10204-5
- Hassan, R., & Ur, S. C. (2020). Synthesis of FeVSb_{1-x}Se_x Half-Heusler Alloys via Mechanical Alloying and Evaluation of Transport and Thermoelectric Properties. *Journal of Electronic Materials*, 49, 5, 2719-2725. doi: 10.1007/s11664-019-07653-1
- Heusler, F. (1903). Über magnetische manganlegierungen. *Verhandlungen der DPG* 5, 219.
- Hill R. (1966) Generalized constitutive relations for incremental deformation of metal crystals by multislip. *J. Mech. Phys. Solid.*, 14, 95-102. doi: 10.1016/0022-5096(66)90040-8
- Huang, L., Zhang, Q., Yuan, B., Lai, X., Yan, X., & Ren, Z. (2016). Recent progress in half-Heusler thermoelectric materials. *Materials Research Bulletin*, 76, 107. doi: 10.1016/J.MATERRESBULL.2015.11.032.
- Hussain, M. K. (2018). Investigations of the electronic and magnetic properties of newly (001) surface LiCrS and LiCrSe half-Heusler compounds. *Applied Physics A* 124, 343. doi: 10.1007/s00339-018-1760-9
- Homes, C. C., Ali, M. N., & Cava, R. J. (2015). Optical properties of the perfectly compensated semimetal WTe₂. *Physical Review B*, 92(16), 161109. doi: 10.1103/PhysRevB.92.161109
- Jain, A., Ong, S. P., Hautier, G., Chen, W., Richards, W. D., Dacek, S., Cholia, S., Gunter, D., Skinner, D., Ceder, G., & Persson, K. (2019). Commentary: the materials project: a materials genome approach to accelerating materials innovation. *APL Materials*, 1, 011002. doi: 10.1063/1.4812323
- Jia, K., Yang, C. L., Wang, M. S., Ma, X. G., & Yi, Y. G. (2021). First-principles investigation on the thermoelectric performance of half-Heusler compound CuLiX (X = Se, Te). *Journal of Physics: Condensed Matter*, 33, 095501. doi: 10.1088/1361-648X/abcdbc
- Jolayemi, O. R., Adetunji, B. I., Ozafire, O. E., & Adebayo, G. A. (2021). Investigation of the thermoelectric properties of Lithium-Aluminium-Silicide (LiAlSi) compound from first-principles calculations. *Computational Condensed Matter*, 27, e00551. Doi: 10.1016/j.cocom.2021.e00551
- Kacimi, S., Mehnane, H., & Zaoui, A. (2014). I-II-V and I-III-IV half-Heusler compounds for optoelectronic applications: Comparative ab initio study. *Journal of Alloys and Compounds*, 587: 451-458. doi: 10.1016/j.jallcom.2013.10.046
- Kandpal, H. C., Felser, C., & Fecher, G. H. (2007). Correlation in Heusler compounds Co₂YSi (Y=3d transition metal). *Journal of Magnetism and Magnetic Materials*, 310(2), 1626-1628. doi: 10.1016/j.jmmm.2006.10.481
- Kilit Dogan, E., & Erden Gulebaglan, S. (2021). Some properties of LiInSi half-Heusler alloy via density functional theory. *Bulletin of Materials Science*, 44, 208. doi: 10.1007/s12034-021-02499-y
- Kilit Dogan, E., & Erden Gulebaglan, S. (2022). A computational estimation on structural, electronic, elastic, optic and dynamic properties of Li₂TlA (A=Sb and Bi): First-principles calculations. *Materials Science in Semiconductor Processing*, 138, 106302. doi: 10.1016/j.mssp.2021.106302
- Kohn, W., & Sham, L. J. (1965). Self-consistent equations including exchange and correlation effects. *Physical Review*, 140, 1133. doi: 10.1103/PhysRev.140.A1133
- Lekhal, A., Benkhelife, F. Z., Meçabih, S., Abbar, B., & Bouhefs, B. (2016). Structural and electronic properties of non-magnetic intermetallic YAUX (X = Ge and Si) in hexagonal and cubic phases. *Bulletin of Materials Science*, 39(1), 195-200. doi: 10.1007/s12034-015-1124-4
- Lin, H., Wray, L. A., Xia, Y., Xu, S., Jia, S., Cava, R. J., Bansil, A., & Hasan, M. Z. (2010). Half-Heusler ternary compounds as new multifunctional experimental platforms for topological quantum phenomena. *Nature Materials*, 9, 546-549. doi: 10.1038/nmat2771

- Ma, T., Yang, C., Xie, Y., Sun, L., Lu, W., Wang, R., & Ren, Y. (2010). First-principles calculations of the structural, elastic, electronic and optical properties of orthorhombic LiGaS₂ and LiGaSe₂. *Physica B: Condensed Matter*, 405(1), 363-368. doi: 10.1016/j.physb.2009.08.091
- Monkhorst, H., & Pack, J. D. (1976). Special points for Brillouin-zone integrations. *Physical Review B*, 13, 5188-5192. doi: 10.1103/PhysRevB.13.5188
- Mouhat, F., & Coudert, F. X. (2014). Necessary and sufficient elastic stability conditions in various crystal systems. *Physical Review B*, 90, 224104. doi: 10.1103/PhysRevB.90.224104
- Nye, F. J. (1995). *Physical properties of crystals their representation by tensors and matrices*. New York: Oxford University Press.
- Perdew, J. P., & Zunger, A. (1981). Self-interaction correction to density-functional approximations for many-electron systems. *Physical Review B*, 23, 5048. doi: org/10.1103/PhysRevB.23.5048
- Perdew, J. P., Burke, K., & Ernzerhof, M. (1997). Generalized Gradient Approximation Made Simple. *Physical Review Letter*, 78, 1396. doi: org/10.1103/PhysRevLett.77.3865
- Reuss A. (1929). Calculation of the flow limits of mixed crystals on the basis of the plasticity of monocrystal. *Z. Angew. Math. Mech.*, 9, 49-58.
- Riffat, S. B., & Ma, X. (2003). Thermoelectrics: A Review of Present and Potential Applications. *Applied Thermal Engineering*, 23, 913-935. doi: 10.1016/S1359-4311(03)00012-7
- Rahman Rano, B., Syed, I. M., & Naqib, S. H. (2020). Ab initio approach to the elastic, electronic, and optical properties of MoTe₂ topological Weyl semimetal. *Journal of Alloys and Compounds*, 829, 154522. doi: org/10.1016/j.jallcom.2020.154522
- Ozdemir, E. G., & Merdan, Z. (2019). First principle predictions on half-metallic results of MnZrX (X= In, Tl, C, Si, Ge, Sn, Pb, N, P, As, Sb, O, S, Se, Te) half-Heusler compounds. *Journal of Magnetism and Magnetic Materials*, 491(1), 165567. doi: 10.1016/j.jmmm.2019.165567
- Telfah, A., Essaound, S. S., Baoziz, H., Charifi, Z., Alsaad, A. M., Ahmad, M. J. A., Hergenröder, R., & Sabirianov, R. (2021). Density Functional Theory Investigation of Physical Properties of KCrZ (Z = S, Se, Te) Half-Heusler Alloys. *Physica Status Solidi B*, 258, 2100039. doi: 10.1002/pssb.202100039
- Vinet, P., Ferrante, J., Smith, J. R., & Rose, J. H. (1986). A universal equation of state for solids. *Journal of Physics C*, 19, L467. doi: 10.1088/0022-3719/19/20/001
- Voigt W. (1889) Ueber die Beziehung zwischen den beiden Elasticitätsconstanten isotroper Körper. *Ann. Phys.*, 274, 573-587.
- Wang, X., Cheng, Z., & Liu, G. (2017). Largest magnetic moments in the half-Heusler alloys XCrZ (X = Li, K, Rb, Cs; Z = S, Se, Te): A first-principles study. *Materials*, 10(9), 1078. doi: 10.3390/ma10091078
- Winterlik, J., Fecher, G. H., Thomas, A., & Fesler, C. (2009). Superconductivity in palladium-based Heusler compounds. *Physical Review B*, 79, 064508. doi: 10.1103/PhysRevB.79.064508
- Yang, J. H., & Stabler, F. R. (2009). Automotive applications of thermoelectric materials. *Journal of Electronic Materials*, 38, 1245-1251. doi: 10.1007/s11664-009-0680-z
- Yang, Z., Liu, Z., Sheng, J., Guo, W., Zeng, Y., Gao, P., & Ye, J. (2017). Opto-electric investigation for Si/organic heterojunction single-nanowire solar cells. *Scientific Reports*, 7, 14575. doi: 10.1038/s41598-017-15300-0
- Yin, L., Gu, C., Zhu, J., Ye, Q., Jiang, E., Wang, W., Liao, M., Yang, Z., Zeng, Y., Sheng, J., Guo, W., Yan, B., Gao, P., Ye, J., & Zhu, Y. (2019). Engineering of hole-selective contact for high-performance perovskite solar cell featuring silver back-electrode. *Journal of Materials Science*, 54, 7789-7797. doi: 10.1007/s10853-018-03258-x
- Zhang, M., Dai, X., Hu, H., Liu, G., Cui, Y., Liu, Z., Wang, J., & Wu, G. (2003). Search for new half-metallic ferromagnets in semi-Heusler alloys NiCrM (M = P, As, Sb, S, Se and Te). *Journal of Physics: Condensed Matter*, 15, 7891-7899. doi: 10.1088/0953-8984/15/46/008
- Zhang, Y., & Xu, X. (2020). Machine learning modeling of lattice constants for half-Heusler alloys. *AIP Advances*, 10, 045121. doi: 10.1063/5.0002448
- Zhang, Y., Zhang, W., Yu, X., Yu, C., Liu, Z., Wu, G., & Meng, F. (2020). The structural, magnetic and electronic properties of Fe-Ni-Ga ternary Heusler alloys. *Materials Science and Engineering: B*, 260, 114654. doi: 0.1016/j.mseb.2020.114654

Zuti, I., Fabian, J., &Sarma, S. D. (2004). Spintronics: Fundamentals and applications. *Reviews of Modern Physics*, 76, 323. doi: 10.1103/RevModPhys.76.323